

Space–Time Duality and the Theory of Temporal Imaging

Brian H. Kolner, *IEEE Member*

Abstract—There exists a beautiful duality between the equations that describe the paraxial diffraction of beams confined in space and the dispersion of narrow-band pulses in dielectrics. We will see that this duality leads naturally to the conclusion that a quadratic phase modulation in time is the analog of a thin lens in space. Therefore, by a suitable combination of dispersion and quadratic phase modulation (now a “time lens”), we can synthesize the time-domain analog of an imaging system. Such a temporal-imaging system can magnify time waveforms in the same manner as conventional spatial-imaging systems magnify scenes. We analyze this space–time duality and derive expressions for the focal length and f -number of a time lens. In addition, the principles of temporal imaging are developed and we derive time-domain analogs for the imaging condition, magnification ratio, and impulse response of a temporal-imaging system.

I. INTRODUCTION

IT IS quite satisfying when the equations that describe two apparently disparate physical phenomena can be cast in nearly identical form so as to shed new light and understanding on each. Such has been the case with the problems of paraxial diffraction [1] and narrow-band dispersion. New understanding (or at least points of view) and even inventions have arisen in the last several decades owing to this fortunate situation. However, in spite of the relative simplicity with which this duality can be arranged, there seems to be a somewhat fragmented treatment of it in the literature (journals and textbooks alike). This paper represents an attempt to fill this void by systematically developing the foundations of the space–time duality between the two problems and deriving the relationships that govern them. As we will see, both problems can be cast in terms of complex parabolic differential equations. In the broadest sense, these are diffusion equations, but the presence of an imaginary coefficient allows for propagation of the envelope functions.

The space–time duality can also be extended to lenses. The application of a quadratic phase modulation to a time waveform is analogous to the action of a thin lens on the transverse profile of a beam. For this so-called “time lens” we can define equivalent expressions for focal length and f -number. By combining a time lens with suitable disper-

sion both before and after the lens, we can create the time-domain analog of an imaging system. A temporal-imaging system based on these principles will allow one to expand or compress (magnify–demagnify) time waveforms while maintaining the overall shape of the envelope. As one would expect, there will emerge from this analysis expressions governing the system magnification and condition for imaging (the time dual of the lens law). In addition, there are limitations to the resolution of a temporal-imaging system. We will see that this arises because of the finite aperture time of any real time lens. Taking advantage of the linearity of the imaging process, this effect is analyzed by deriving the impulse response of a temporal-imaging system. Finally, in spite of the exciting possibilities, space does not permit a full discussion of applications of temporal imaging. Many can be found in the references cited and the rest we leave to the imagination of the reader.

There were two important trends in the optical community that led to the current view of temporal imaging. The first was the vigorous development of pulse-compression techniques based largely on the principles of chirp radar [2]. The key elements of this technology are mechanisms for the chirping and spectral broadening of waveforms combined with group delay dispersion for subsequent compression. In the early days, attention was focused on spectral broadening using electrooptic modulators in conjunction with dispersive delay lines in the form of resonant atomic vapors [3]–[6]. We call this “active pulse compression” since it relies on supplying power to the chirping mechanism. With the invention of the diffraction grating-pair dispersive delay line [7] in combination with spectral broadening (chirping) by self-phase modulation in optical fibers [8], passive pulse compression became one of the key links in the race to the world’s shortest optical pulse [9]. However, in recent years, there has been renewed interest in using electrooptic modulators for chirping optical waveforms and several groups have used them for waveform manipulation [10], [11] and active pulse compression [12], [13].

The other important trend was the observation of a mathematical duality between the equations of paraxial (Fresnel) diffraction and narrow-band dispersion. This was pointed out by Akhmanov *et al.* in a general treatment of second- and third-order nonlinear optical interactions [14], [15]. The extension of this duality to include lenses, and hence, imaging was discussed from a systems

Manuscript received June 11, 1993; revised November 12, 1993. This work was supported in part by the National Science Foundation under Grant ECS 9110678 and by the David and Lucile Packard Foundation.

The author is with the Department of Electrical Engineering, University of California, Los Angeles, CA 90024.

IEEE Log Number 9402331.

point of view by Papoulis [16]. Similar ideas have also been discussed by Telegin and Chirkin [17] and Akhmanov [18], who all described the mathematical possibilities of temporal imaging and discussed some of its potential features such as time reversal and time-scale alteration. Later, Kolner and Nazarathy [19] described a complete imaging configuration with design guidelines based on equivalent expressions for focal length, f -number, and magnification, and suggested several applications for temporal imaging.

As a matter of historical record, the need for more-advanced radar signal processing led to an innovation that apparently predates all of the similar work done in optics and was the first demonstration of temporal imaging, conducted in a purely electrical system [20]. Developed by Caputi, who coined the name "Stretch," it is a technique for altering the time scale of electrical waveforms by using the same principles as chirp radar, but organized in a way that exactly parallels conventional imaging. The fact that it has gone largely unnoticed by the optical community is perhaps because the author did not cast the theory in the framework of its spatial counterpart. As we will see in the following sections, the spatial analog provides a powerful and intuitive way of understanding time-scale transformation.

II. OVERVIEW

The foundation of temporal imaging lies in the duality between the problems of paraxial diffraction and narrow-band dispersion and is constructed by two straightforward approximations to the wave equation. Schematically, we can organize the approach as shown in Fig. 1. The wave equation for the electric or magnetic field is constructed from Maxwell's equations in the usual way. The most general solution to the wave equation yields a description of the space-time evolution of an arbitrarily shaped wave function and is quite difficult to obtain. We are therefore left with the task of making approximations that will render the wave equation exactly solvable. In general, we choose to concentrate on either the spatial or temporal evolution of the wave function.

In studying the spatial problem we first assume that the frequency spectrum of the wave is monochromatic. Thus, there is only harmonic time variation and time derivatives in the wave equation become multiplicative constants ($\partial/\partial t \rightarrow i\omega$). In addition, we allow variation in the transverse spatial structure to the extent that wave propagation is mostly in one direction and initially bounded in the vicinity of the axis along which it propagates. This is the so-called paraxial approximation and results in a parabolic partial differential equation for the evolution of the transverse profile of the wave or "beam." For a z -directed beam, the total electric field will therefore take the form

$$\mathbf{E}(x, y, z, t) = E(x, y, z)e^{i(\omega_0 t - k(\omega_0)z)} \quad (1)$$

where $E(x, y, z)$ is a slowly varying envelope function for the transverse beam profile.

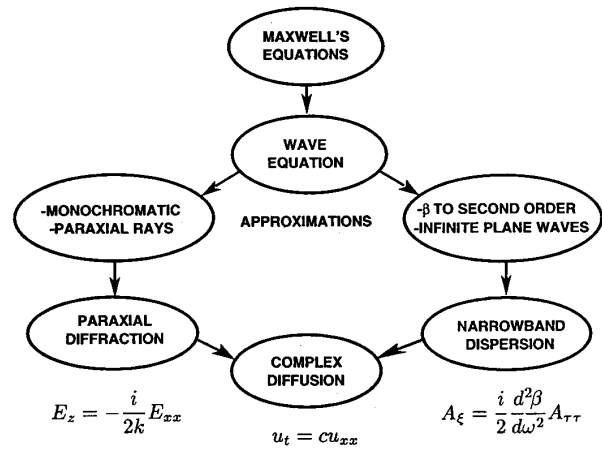


Fig. 1. The derivation of the paraxial diffraction and narrow-band dispersion problems through complementary approximations to the wave equation. Resulting parabolic differential equations can be viewed as complex diffusion equations.

The temporal problem is approached in a similar fashion, but now we invoke a complementary set of approximations. Since we are interested in describing the evolution of pulses, or modulated waves in general, we may no longer assume a monochromatic field. However, if we limit the temporal-frequency spectrum to a suitable range, then the propagation of any spectral component within the wave can be accounted for by a Taylor-series expansion of the propagation constant $\beta(\omega)$ to second order in ω . We may also ignore the spatial profile of the wave and approximate it as an infinite plane wave. These two approximations simplify the wave equation and result in a parabolic differential equation for the space-time evolution of the pulse envelope or "wave packet." The total electric field for this problem can then be represented as

$$\mathbf{E}(x, y, z, t) = A(z, t)e^{i(\omega_0 t - \beta(\omega_0)z)} \quad (2)$$

where $A(z, t)$ is a slowly varying envelope function that describes a wave packet propagating in the z -direction.

It is interesting to note from the foregoing discussion that a duality exists between the complementary approximations leading to the two problems. This is highlighted in Fig. 2, where we consider the spatial- and temporal-frequency spectra appropriate to each problem. For paraxial diffraction the assumption of monochromaticity leads to a delta function in the temporal-frequency spectrum at the carrier frequency $\omega = \omega_0$. The paraxial nature of the spatial profile implies a narrow band of spatial frequencies centered about $k_x = k_y = 0$ for a z -directed beam [Fig. 2(a)].

For the dispersion problem, the temporal structure (e.g., pulses) yields a finite, yet narrow band of temporal frequencies. The assumption that the wave is an infinite plane wave demands that there be a spatial form of monochromaticity; that is, the spatial frequency spectrum will be a delta function at $k_x = k_y = 0$ [Fig. 2(b)].

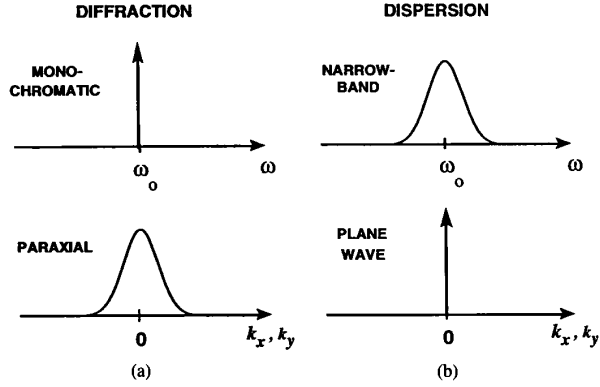


Fig. 2. Duality between the approximations used to derive (a) the paraxial diffraction and (b) narrow-band dispersion problems.

III. PARAXIAL DIFFRACTION

To derive the equation governing paraxial diffraction, we start with Maxwell's equations and apply the standard techniques of vector calculus to arrive at the wave equation for the electric field

$$\nabla^2 \mathbf{E} = \mu \epsilon \frac{\partial^2 \mathbf{E}}{\partial t^2} \quad (3)$$

where, without loss of generality, we take the field to be a scalar function of position. To study the paraxial diffraction problem, we first make the simplifying assumption that the wave is monochromatic

$$\mathcal{E}(x, y, z, \omega) = \mathbf{E}_0(x, y, z) \delta(\omega - \omega_0) \quad (4)$$

so that the wave equation is reduced to the Helmholtz equation

$$(\nabla^2 + k^2) \mathbf{E}_0 = 0 \quad (5)$$

where

$$k^2 = \mu \epsilon \omega_0^2 = \left(\frac{2\pi}{\lambda} \right)^2. \quad (6)$$

Now, we want to study this equation for paraxial rays, i.e., rays confined mostly along the z -axis. Thus, the most rapid phase variation will occur along the z -axis and we can explicitly identify this dependence by writing

$$\mathbf{E}_0(x, y, z) = E(x, y, z) e^{-ikz} \quad (7)$$

where $E(x, y, z)$ is an envelope function that varies slowly compared to the wavenumber k .

Using the above form for \mathbf{E}_0 in the Helmholtz equation results in the reduced wave equation

$$\frac{\partial^2 E}{\partial x^2} + \frac{\partial^2 E}{\partial y^2} + \frac{\partial^2 E}{\partial z^2} - 2ik \frac{\partial E}{\partial z} = 0. \quad (8)$$

Next, we invoke the paraxial approximation

$$\left| \frac{\partial^2 E}{\partial z^2} \right| \ll \begin{cases} \left| \frac{\partial^2 E}{\partial x^2} \right| \\ \left| \frac{\partial^2 E}{\partial y^2} \right| \\ \left| 2k \frac{\partial E}{\partial z} \right|. \end{cases} \quad (9)$$

In physical terms, this approximation says that the curvature of the field envelope in the direction of propagation (owing to diffractive spreading) is much less than the curvature of the transverse profile. The result is the "paraxial wave equation"

$$\frac{\partial^2 E}{\partial x^2} + \frac{\partial^2 E}{\partial y^2} - 2ik \frac{\partial E}{\partial z} = 0 \quad (10)$$

which can also be written in more compact form as

$$\frac{\partial E}{\partial z} = -\frac{i}{2k} \nabla_t^2 E \quad (11)$$

where ∇_t^2 is the transverse Laplacian operator, or

$$E_z = -\frac{i}{2k} (E_{xx} + E_{yy}) \quad (12)$$

where the subscripts on the field amplitudes imply partial differentiation with respect to that coordinate.

Equations (10)–(12) govern the evolution of the electric-field envelope as the beam propagates down the z -axis. This equation is of parabolic form, similar to the heat diffusion equation, but with an imaginary coefficient. In the next section, we will see that a similar equation governs the dispersion problem as well. By applying the known solutions of the diffusion problem to the wave problems, we can immediately arrive at the behavior of diffraction and dispersion which, not surprisingly, will exhibit spreading like a temperature distribution, but for different reasons.

IV. NARROW-BAND DISPERSION

Next, we wish to construct a differential equation that describes the evolution of the electric-field envelope $A(z, t)$ of a narrow-band z -directed plane wave propagating in a medium with propagation constant $\beta(\omega)$ [viz. (2)]. Haus [21] has shown that this is possible by first finding a differential equation for an arbitrary spectral component $\mathcal{A}(z, \omega - \omega_0)$ and then superposing all components of the spectrum $\mathcal{A}(z, \omega)$. Assuming that the bandwidth of $\mathcal{A}(z, \omega)$ is small and centered around ω_0 , we can expand $\beta(\omega)$ to second order in ω and the equation for $\mathcal{A}(z, \omega - \omega_0)$ can be shown to be

$$\frac{\partial \mathcal{A}(z, \omega - \omega_0)}{\partial z} = -i \left[(\omega - \omega_0) \frac{d\beta}{d\omega} + \frac{(\omega - \omega_0)^2}{2} \frac{d^2\beta}{d\omega^2} \right] \mathcal{A}(z, \omega - \omega_0). \quad (13)$$

Inverse Fourier transformation then leads to the desired equation for $A(z, t)$

$$\left(\frac{\partial}{\partial z} + \frac{1}{v_g} \frac{\partial}{\partial t} \right) A(z, t) = \frac{i}{2} \frac{d^2\beta}{d\omega^2} \frac{\partial^2 A(z, t)}{\partial t^2} \quad (14)$$

where $v_g = (d\omega/d\beta)$. (An interesting alternative derivation of (14) is given by Siegman [22]). This equation can be further simplified by introducing a change of variables to a traveling-wave coordinate system:

$$\begin{aligned} \tau &= (t - t_o) - \left(\frac{z - z_o}{v_g} \right) \\ \xi &= z - z_o \end{aligned} \quad (15)$$

where t_o and z_o are arbitrary references. Then, (14) takes on the more useful form

$$\frac{\partial A(\xi, \tau)}{\partial \xi} = \frac{i}{2} \frac{d^2\beta}{d\omega^2} \frac{\partial^2 A(\xi, \tau)}{\partial \tau^2} \quad (16)$$

which we recognize as being similar to the paraxial wave equation. This traveling-wave form is particularly convenient because the solution gives the pulse evolution "centered" on the envelope ($\tau = 0$) moving at the group velocity v_g using the propagation distance ξ as a parameter.

V. THE DIFFUSION EQUATION

We have seen how the complementary approximations to the wave equation yield new equations for the envelope functions of paraxial diffraction and narrow-band dispersion. We transformed what was initially a hyperbolic equation into one of a pair of parabolic equations that we would normally associate with diffusion. However, these new equations have imaginary coefficients, and therefore, are wave equations for linear dispersive waves [23] (also called Schrödinger equations). The imaginary coefficients introduce a new richness into classical diffusion. They allow, for example, the possibility for the envelope function to propagate. At the same time, the strong similarities to diffusion invite a closer look at the relationship between the two systems. Thus, we digress briefly to examine the nature of the diffusion equation, its solution, and the implications for "complex diffusion equations."

The general form of the two-dimensional diffusion equation in a source-free region can be written

$$u_t = c\nabla^2 u \quad (17)$$

where c is a constant known as the *diffusivity* of the medium. For the problem of heat diffusion, this constant is

$$c = \frac{\kappa}{C\rho} \quad (18)$$

where κ is the thermal conductivity, C is the specific heat, and ρ is the density. There is a simple physical interpretation to the diffusion equation (17). It says that the rate of

change of the temperature $u(\mathbf{r}, t)$ at a point \mathbf{r} is proportional to the product of the diffusivity c and the local "curvature" of the temperature distribution. That is, the more tightly confined the thermal energy, the more rapidly it diffuses into adjacent regions. We know this to be true also for the case of diffraction. The more tightly confined a beam is with respect to a wavelength, the more rapidly the beam diffracts as it propagates. The same applies to the dispersion equation. The shorter the pulse envelope, and hence the local curvature, the faster it spreads out.

To examine what is behind this common behavior, we first list the three equations in simplified form:

$$\begin{aligned} u_t &= cu_{xx} && \text{heat diffusion} \\ E_z &= -\frac{i}{2k} E_{xx} && \text{paraxial diffraction} \\ A_\xi &= \frac{i}{2} \frac{d^2\beta}{d\omega^2} A_{\tau\tau} && \text{narrow-band dispersion} \end{aligned} \quad (19)$$

Here we have written only the one-dimensional form of the heat and diffraction equations to emphasize the similarity to dispersion. All three problems are governed by the same parabolic differential equation and therefore must have solutions of identical form. Using heat diffusion as a model, it can be shown that the general solution to the one-dimensional diffusion equation is [24]

$$u(x, t) = \frac{1}{2\pi} \int_{-\infty}^{\infty} F(k_x, 0) e^{-ck_x^2 t} e^{ik_x x} dk_x \quad (20)$$

where $F(k_x, 0)$ is the spatial Fourier spectrum of the initial distribution $u(x, 0)$ and k_x is the Fourier-domain variable with units of meter⁻¹. The analysis is readily extended to the case of two dimensions with the result

$$\begin{aligned} u(x, y, t) &= \frac{1}{(2\pi)^2} \iint_{-\infty}^{\infty} F(k_x, k_y, 0) \\ &\quad \cdot e^{-c(k_x^2 + k_y^2)t} e^{i(k_x x + k_y y)} dk_x dk_y. \end{aligned} \quad (21)$$

The solution, in this form as an integral equation, also has a simple physical interpretation. The initial spectrum $F(k_x, k_y, 0)$ is modified by an exponential filter function $\exp[-c(k_x^2 + k_y^2)t]$. When the coefficient c is real, the filter is of Gaussian low-pass form with a bandwidth that decreases with time [Fig. 3(a)]. The reduction in bandwidth necessarily results in a broadening or smoothing out of the temperature distribution, a fact confirmed by experience.

To apply this result to the two wave equations, we simply exchange the independent variables and diffusivity terms. For two-dimensional diffraction we let

$$\begin{aligned} t &\rightarrow z \\ c &\rightarrow -\frac{i}{2k} \end{aligned} \quad (22)$$

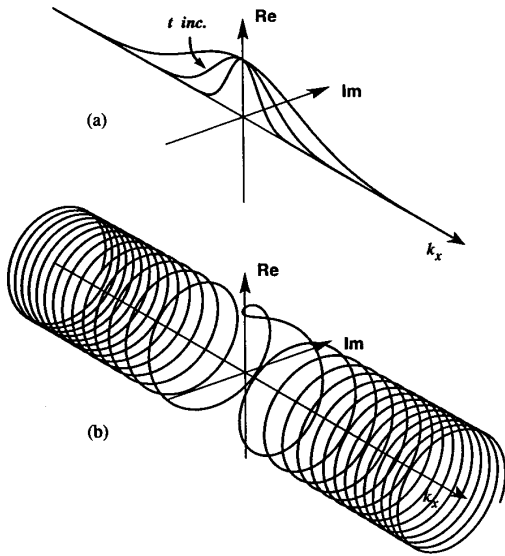


Fig. 3. Frequency-domain filter functions for parabolic differential equations. (a) For heat diffusion, filter is of Gaussian low-pass form with bandwidth decreasing with time. (b) For diffraction or dispersion, spectrum is multiplied by a quadratic phase function with phase slope that increases with time (the temporal nature of this change is not shown).

to obtain

$$E(x, y, z) = \frac{1}{(2\pi)^2} \iint_{-\infty}^{\infty} \mathcal{E}(k_x, k_y, 0) \cdot e^{i(k_x^2 + k_y^2)z/2k} e^{i(k_x x + k_y y)} dk_x dk_y \quad (23)$$

where again $\mathcal{E}(k_x, k_y, 0)$ is the initial Fourier spectrum. For the dispersion problem, we similarly let

$$\begin{aligned} t &\rightarrow \xi \\ c &\rightarrow \frac{i}{2} \frac{d^2\beta}{d\omega^2} \end{aligned} \quad (24)$$

and find

$$A(\xi, \tau) = \frac{1}{2\pi} \int_{-\infty}^{\infty} \mathcal{A}(0, \omega) e^{-i\frac{\xi}{2} \frac{d^2\beta}{d\omega^2} \omega^2} e^{i\omega\tau} d\omega. \quad (25)$$

So, the solutions to the wave-propagation problems are found by multiplying the initial spectra by a phase term quadratic in frequency and linear in the propagation variable. The effect is to introduce a spiral or “corkscrew” into the complex Fourier spectrum [Fig. 3(b)]. Fig. 4 depicts this effect on an initially Gaussian amplitude spectrum as it propagates. Note how the phase winds symmetrically from the middle of the spectrum as the beam advances. A straightforward Fourier transformation of the spectrum shows that the corresponding real-space picture is one of a beam expanding laterally and acquiring a spatial “chirp.” This is also the picture that one obtains by taking a planar slice through a spherical wavefront and measuring the electric field in the plane.

The quadratic phase term can also be viewed as producing a filtering effect consistent with a stationary-phase

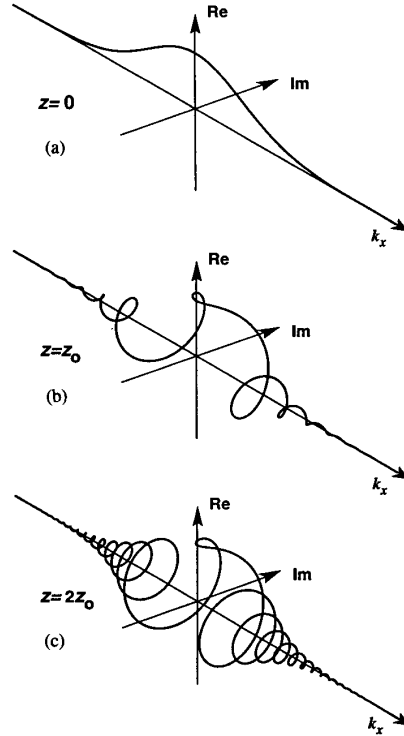


Fig. 4. Complex spatial-frequency spectrum of a Gaussian beam undergoing diffraction. (a) Initial spectrum. (b) Spectrum after propagating a distance $z = z_0$. (c) Spectrum after propagating a distance $z = 2z_0$.

point of view. As the beam propagates, the increase in rapid phase oscillations in the higher frequencies will tend to wash out their contribution upon superposition in the Fourier integral. This will necessarily lead to a spreading out of the real-space field envelope. It is important to realize that dispersion and diffraction do not alter the magnitude of the Fourier spectra (they are, after all, dissipationless phenomena). They merely rearrange the phase of the initial spectrum. In contrast, real diffusion attenuates the high-frequency components.

VI. SPACE LENSES AND TIME LENSES

Having shown that dispersion can be viewed as the time-domain analog of paraxial diffraction, we now proceed to find a time-domain analog to a space lens. Consider the standard thin lens portrayed in Fig. 5(a). We know that the effect of a thin lens can be described by a phase transformation of the form [25]

$$t_l(x, y) = \exp[-ikn\Delta_0] \exp\left[i\frac{k}{2f}(x^2 + y^2)\right] \quad (26)$$

(assuming $\exp(+i\omega_0 t)$ time dependence) where Δ_0 is the maximum thickness and f is the focal length containing the usual physical properties of the lens such as the radii of curvature (R_1 and R_2) of the two surfaces and the

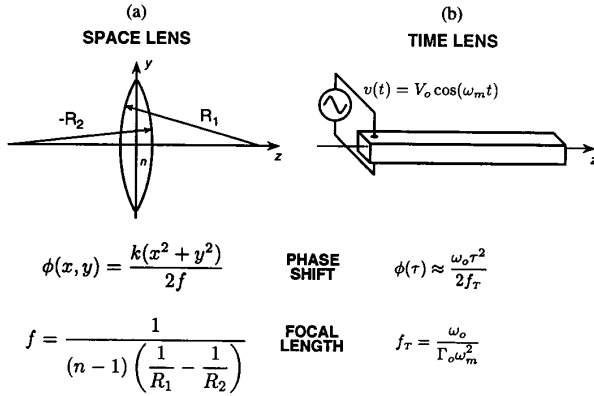


Fig. 5. (a) Conventional space lens with phase function defined in terms of focal length, which in turn depends on surface curvature and index of refraction. (b) Time lens implemented with a traveling-wave electrooptic modulator driven at a microwave frequency ω_m . Phase function is defined in terms of a focal time f_T , which depends on the optical carrier frequency ω_o , the modulation index Γ_o , and ω_m .

index of refraction n . The first term in (26) is a simple phase shift and can be ignored for the purposes of this discussion. The second term contains the essence of lens operation. It shows that a lens produces an *instantaneous quadratic phase modulation in real space* (as opposed to the quadratic phase modulation produced in Fourier space by diffraction). The relevant spatial-phase function is thus

$$\phi(x, y) = \frac{k(x^2 + y^2)}{2f}. \quad (27)$$

Now, in order to find the time-domain equivalent of the space lens, we look to the governing parabolic equations (19) for guidance. Since a space lens produces a quadratic phase modulation on the *profile variables* (x, y) , it suggests that we do the same in the time domain. In other words, produce a quadratic phase modulation on the local time variable τ . We could describe this functionally as $\phi(\tau) = \mu\tau^2$ where μ is a constant, or, in keeping with the spirit of the space-time duality, let us write

$$\phi(\tau) = \frac{\omega_o \tau^2}{2f_T} \quad (28)$$

where f_T is the "focal time" of the "time lens." This time-phase function is then the dual of its spatial counterpart (27).

We can find a general expression for the focal time of a time lens realized by any physical process by comparing (28) to a Taylor-series expansion of the phase function

$$\begin{aligned} \phi(\tau) = \phi_o(\tau_o) + (\tau - \tau_o) \left. \frac{d\phi}{d\tau} \right|_{\tau=\tau_o} \\ + \frac{(\tau - \tau_o)^2}{2!} \left. \frac{d^2\phi}{d\tau^2} \right|_{\tau=\tau_o} + \dots \quad (29) \end{aligned}$$

Equating the second-order term (with $\tau_o = 0$) to (28) we find

$$f_T = \frac{\omega_o}{d^2\phi/d\tau^2}. \quad (30)$$

To obtain a more specific relationship, we need to examine a particular physical mechanism for producing quadratic phase modulation. Electrooptic phase modulation is a prime candidate [Fig. 5(b)] since it can produce a reliable phase modulation independent of optical power (this would not be the case for self-phase modulation, which depends on the optical power and pulse shape). We will therefore examine the operation of electrooptic phase modulators with emphasis on relating the quadratic phase to the properties of time lenses.

In a traveling-wave phase modulator driven with a voltage $v(t) = V_o \cos \omega_m t$, any optical wave that is mostly confined to a region beneath a cusp of the traveling-wave field will receive a quadratic phase modulation or retardation compared to the same optical path in the absence of the modulating field. The effect can be viewed as being produced by a traveling-wave modulation of the index of refraction (and hence, the optical path length through the crystal).

The total phase shift of an optical wave propagating through an electrooptic crystal with a traveling-wave index of refraction $\Delta n(z, t)$ can be written as

$$\begin{aligned} \phi(z, t) = \omega_o t - k_o z - \frac{\omega_o}{c} \int_0^z \Delta n(z', t) dz' \\ = \omega_o t - k_o z - \Gamma(z, t) \quad (31) \end{aligned}$$

where the last term accounts for the phase retardation due to electrooptic interaction with a microwave driving field and

$$\Delta n(z, t) = \Delta n_o \cos(\omega_m t - k_m z + \theta). \quad (32)$$

Here Δn_o is the peak index of refraction change, ω_m is the frequency of the microwave driving field, k_m is the microwave wavenumber, and θ is the initial phase offset.

Once again it will be advantageous to cast this integral in the traveling-wave coordinate system of the optical fields. To this end we invoke the transformation indicated in (15) and apply it to the integral in (31). The net retardation is therefore [26]

$$\begin{aligned} \Gamma(\xi, \tau) = \frac{\omega_o}{c} \int_0^\xi \Delta n(\xi', \tau) d\xi' = \frac{\omega_o}{c} \int_0^\xi \Delta n_o \\ \cdot \cos \left[\omega_m \left(\tau + \xi \left(\frac{1}{v_{go}} - \frac{1}{v_{pm}} \right) + \frac{\theta}{\omega_m} \right) \right] d\xi' \\ = \Gamma_o \frac{\sin \left(\frac{\Delta\phi}{2} \right)}{\left(\frac{\Delta\phi}{2} \right)} \cos \left(\frac{\Delta\phi}{2} + \omega_m \tau + \theta \right) \quad (33) \end{aligned}$$

where

$$\Delta\phi = \omega_m \xi \left(\frac{1}{v_{go}} - \frac{1}{v_{pm}} \right) \quad (34)$$

is the phase offset due to walkoff between the optical group velocity v_{go} and the microwave phase velocity v_{pm} and Γ_o is the peak phase deviation in the absence of velocity walkoff. Γ_o depends on the peak applied electric field, the electrooptic coefficients, and the total propagation distance ξ . In terms of the peak index change Δn_o or the half-wave switching voltage V_π , it takes the form

$$\Gamma_o \equiv \frac{\omega_o \Delta n_o \xi}{c} = \pi \frac{V}{V_\pi}. \quad (35)$$

The above analysis applies only to the case of a traveling-wave modulator with copropagating microwave and optical fields. For a standing-wave (resonant) modulator, we need to consider the effect of the counterpropagating field on the net retardation. This is easily taken into account by reversing the sign of the wavenumber ($k_m \rightarrow -k_m$) in (32) and adding an additional phase to satisfy the boundary condition $\Delta n(z=0) = 0$. The net retardation now has two terms corresponding to the forward and backward traveling waves, respectively;

$$\begin{aligned} \Gamma(\xi, \tau) &= \Gamma_o \left\{ \frac{\sin\left(\frac{\Delta\phi}{2}\right)}{\left(\frac{\Delta\phi}{2}\right)} \cos\left(\frac{\Delta\phi}{2} + \omega_m \tau + \theta\right) \right. \\ &\quad \left. - \frac{\sin\left(\frac{\eta}{2}\right)}{\left(\frac{\eta}{2}\right)} \cos\left(\frac{\eta}{2} + \omega_m \tau + \theta\right) \right\} \\ &= \Gamma_+(\xi, \tau) + \Gamma_-(\xi, \tau) \end{aligned} \quad (36)$$

where

$$\eta = \omega_m \xi \left(\frac{1}{v_{go}} + \frac{1}{v_{pm}} \right). \quad (37)$$

Large values of η correspond to the optical pulse propagating through many cycles of counterpropagating microwave field, each one canceling the effect of the previous one. This results in "washing out" the backward modulation effect when compared to the growth due to the forward wave, as seen in the term $\sin(\eta/2)/(\eta/2)$. It would seem to argue, then, for long interaction lengths. However, it is interesting to note what occurs for perfect velocity matching in a resonant microwave cavity with a total length equal to an arbitrary integral number of half wavelengths. Since $v_{pm} = v_{go}$, then

$$\frac{\eta}{2} = \frac{\omega_m \xi}{v_{pm}} = k_m \xi \quad (38)$$

and the retardation produced by the backward propagating wave is given by

$$\Gamma_-(\xi, \tau) = -\frac{\sin(k_m \xi)}{(k_m \xi)} \cos(k_m \xi + \omega_m \tau + \theta). \quad (39)$$

Now, for a resonator constructed with an integral number of half wavelengths in the direction of optical propagation $k_m \xi = N\pi$ and thus

$$\Gamma_-(\xi, \tau) = 0 \quad v_{pm} = v_{go}. \quad (40)$$

Thus, for a resonant microwave phase modulator with perfect velocity matching, there is no electrooptic retardation either positive or negative due to the counterpropagating field.

Let us now return to the matter of the analogous properties between time and space lenses. For the remainder of this section, we will assume a time lens that has perfect velocity matching ($\Delta\phi = 0$), no initial phase offset ($\theta = 0$), and no coupling to a backward wave. The net retardation is then given by

$$\Gamma(\xi, \tau) = \Gamma_o \cos(\omega_m \tau). \quad (41)$$

In order to have a lens effect, we need to isolate that portion of the modulation that results in a quadratic phase transformation. This is accomplished by restricting the duration of the optical pulse (or waveform) to a small region about $|\tau| = 0$. Then we can expand the cosine function and

$$\Gamma(\xi, \tau) \approx \Gamma_o \left[1 - \frac{(\omega_m \tau)^2}{2} \right]. \quad (42)$$

The leading term is a simple static phase shift and does not play an important role. It is equivalent to the static phase term in (26) due to the optical path through the center of a lens. Now, if we compare the quadratic term in (42) to the assumed form of the time-lens phase (28), or, equivalently, use the general definition (30), we arrive at an expression for the temporal focal length or "focal time"

$$f_\tau = \frac{\omega_o}{\Gamma_o \omega_m^2}. \quad (43)$$

Thus, we can characterize the time lens by an instantaneous phase transformation

$$\begin{aligned} H_i(\tau) &= \exp[-i\Gamma_o] \exp\left[i\frac{\Gamma_o(\omega_m \tau)^2}{2}\right] \\ &= \exp[-i\Gamma_o] \exp\left[i\frac{\omega_o \tau^2}{2f_\tau}\right]. \end{aligned} \quad (44)$$

Continuing the analogy, we next seek an appropriate description of f -number. In conventional optics, this is the ratio of focal length to aperture size. Inasmuch as the aperture size dictates the maximum usable area of the lens, we can extend this concept to the time lens by defining the maximum usable time window as that portion of the phase modulation that is predominantly quadratic. If we expand (41) to the next higher order (fourth) and require that within some time window $|\tau| \leq \tau_a/2$ this term be less than, say, 2 percent of the quadratic term,

then the maximum usable time aperture becomes

$$\tau_a \approx 1/\omega_m. \quad (45)$$

If we now define the f -number as the ratio of the focal time f_T to the aperture time τ_a we have

$$f_T^\# \equiv \frac{f_T}{\tau_a} = \frac{\omega_o}{\Gamma_o \omega_m}. \quad (46)$$

Although the condition of 2 percent contribution from the fourth-order term seems arbitrary, it was found in earlier studies of active pulse compression [12] that ratios of $T/\tau_a < 6$ (where T is the microwave period) produced objectionable distortion of the input pulses. The condition set forth in (45) is slightly more conservative and corresponds to $T/\tau_a = 2\pi$.

We may now start to formally organize the dualities between diffraction and dispersion and space lenses and time lenses. Table I displays the pertinent equations for both problems. To this point we have seen that the governing partial differential equations for both systems are identical. The "propagation variable" can be viewed as the independent parameter that measures the distance of propagation. It was arbitrarily chosen as the z -axis for both the diffraction and the dispersion problems. The profile variable is the coordinate direction in which the main feature of the wave is modified upon propagation. For diffraction this is the plane transverse to the direction of propagation, while for dispersion, it is the local time centered about the pulse envelope. The diffusivity measures the rate at which the wave profile changes as it propagates. This term is imaginary, and thus, only contributes to the phase of the wave's spectrum. Note that in diffraction this can have only one sign, while for the case of dispersion we can find materials or synthesize optical paths for which $d^2\beta/d\omega^2$ is either greater or less than zero. As we shall see, this will permit an extra degree of freedom when designing temporal-imaging systems.

Finally, by considering the fundamental action of space lenses, we arrived at a time-domain analog: the time lens. Its properties could be characterized in terms of a focal time and f -number. These concepts carry over directly from their space counterparts and take their respective places in Table I. The remaining entries will be described in the next sections.

VII. TEMPORAL IMAGING

Now that we have derived the time-domain analogs to diffraction and lenses, it is natural to consider putting them together in a system. In the space domain, the combination of a lens and suitable distance for diffraction so that a beam is focused to a spot is analogous to pulse compression in time. More precisely, the signal obtained in the focal plane of a time lens will be the Fourier transform of the input signal. The first and perhaps most-famous system application based on this principle was chirp radar [2].

A much more powerful system configuration is obtained

TABLE I
THE EQUATIONS OF SPATIAL AND TEMPORAL IMAGING. ENTRIES FOR THE IMPULSE RESPONSE INDICATE FOURIER TRANSFORMS OF PUPIL FUNCTIONS

	SPACE	TIME
Governing p.d.e.	$E_z = -\frac{i}{2k}(E_{xx} + E_{yy})$	$A_\xi = \frac{i}{2} \frac{d^2\beta}{d\omega^2} A_{\tau\tau}$
Propagation variable	z	ξ
Profile variable	x, y	τ
Diffusivity	$-\frac{i}{2k}$	$\frac{i}{2} \frac{d^2\beta}{d\omega^2}$
Lens phase function	$\phi(x) = \frac{k(x^2 + y^2)}{2f}$	$\phi(t) = \frac{\omega_o \tau^2}{2f_T}$
Focal length (time)	$f = \frac{1}{(n-1)\left(\frac{1}{R_1} - \frac{1}{R_2}\right)}$	$f_T = \frac{\omega_o}{\Gamma_o \omega_m}$
f -number	$f^\# = \frac{f}{d}$	$f_T^\# = \frac{\omega_o}{\Gamma_o \omega_m}$
Imaging condition	$\frac{1}{d_o} + \frac{1}{d_i} = \frac{1}{f}$	$\frac{1}{\xi_1} \frac{d^2\beta_1}{d\omega^2} + \frac{1}{\xi_2} \frac{d^2\beta_2}{d\omega^2} = -\frac{\omega_o}{f_T}$
Magnification	$M = -\frac{d_i}{d_o}$	$M = -\frac{\xi_2 \frac{d^2\beta_2}{d\omega^2}}{\xi_1 \frac{d^2\beta_1}{d\omega^2}}$
Impulse response (essential feature)	$\mathcal{F}\{P(\lambda d_i \bar{x}, \lambda d_i \bar{y})\}$	$\mathcal{F}\left\{P\left(\xi_2 \frac{d^2\beta_2}{d\omega^2} \bar{\tau}\right)\right\}$

by preceding *and* following a time lens with dispersion [Fig. 6(a)]. When the magnitudes of the pre- and post-dispersion are suitably chosen with respect to the characteristics of the time lens, a "temporal imaging system" is created [16]–[20]. By this we mean that the output waveform from the system is a scaled replica of the input waveform; stretched or compressed in time with a concomitant scaling in power to satisfy energy conservation.

In order to characterize the temporal-imaging system, we will make use of the fact that the system is linear in electric-field amplitude and use standard linear-systems techniques where they are advantageous. Recall that the principle feature of the solution to the dispersion problem is that the input spectrum is multiplied by a phase-shift term quadratic in the Fourier variable (ω). Also, the effect of the time lens is to multiply the time-dependent electric field by a phase-shift term quadratic in the time variable. The output of the system is thus found by cascading the three effects [Fig. 6(b)].

Fig. 7 displays the identical analysis applied to a spatial-imaging system. Here, the quadratic phase is applied in the spatial Fourier domain that describes the diffraction phenomenon and in real space to describe the action of a lens.

Now, consider an arbitrary waveform entering the temporal imaging system of Fig. 6. To simplify future calculations, we group all of the important time- and frequency-domain functions in Table II. In traveling-wave coordinates, the waveform envelope is $\mathcal{A}(\xi, \tau)$ with associated

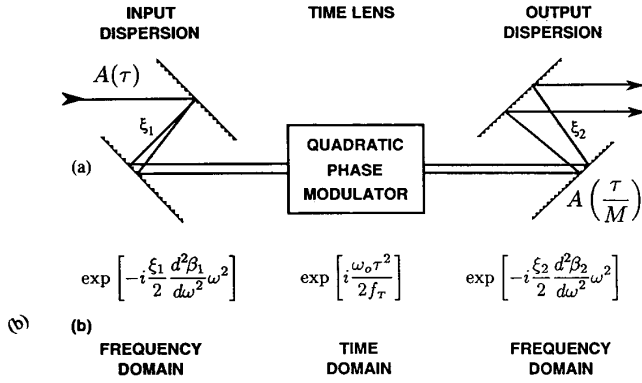


Fig. 6. (a) Temporal-imaging configuration. Input and output dispersions (shown here as diffraction-grating pairs) play the role of free-space diffraction while a quadratic phase modulator acts as a lens in the time domain. Output waveform envelope $A(\tau/M)$ is a magnified version of the input envelope $A(\tau)$, where $M \equiv -(\xi_2 d^2 \beta_2 / d \omega^2) / (\xi_1 d^2 \beta_1 / d \omega^2)$. (b) Analysis is carried out by cascading the three processes: input dispersion [quadratic phase transformation in frequency domain (ω)] \rightarrow time lens [quadratic phase modulation in time (τ)] \rightarrow output dispersion. Compare with the spatial analog shown in Fig. 7.

TABLE II
TIME- AND FREQUENCY-DOMAIN FUNCTIONS CORRESPONDING TO THE PHENOMENON OF DISPERSION AND THE ACTION OF A TIME LENS IN A TEMPORAL-IMAGING SYSTEM

	TIME	FREQUENCY	
INPUT			
DISPERSION	$G_1(\xi_1, \tau) = \frac{1}{\sqrt{4\pi i a}} \exp\left(i \frac{\tau^2}{4a}\right)$	$G_1(\xi_1, \omega) = \exp(-i\omega^2)$	$a = \frac{\xi_1 d^2 \beta_1}{2 d \omega^2}$
OUTPUT			
DISPERSION	$G_2(\xi_2, \tau) = \frac{1}{\sqrt{4\pi i b}} \exp\left(i \frac{\tau^2}{4b}\right)$	$G_2(\xi_2, \omega) = \exp(-i\omega^2)$	$b = \frac{\xi_2 d^2 \beta_2}{2 d \omega^2}$
TIME LENS	$H(\tau) = \exp\left(i \frac{\tau^2}{4c}\right)$	$\mathcal{H}(\omega) = \sqrt{4\pi i c} \exp(-i\omega^2)$	$c = \frac{f_r}{2\omega_0}$

frequency spectrum $\mathcal{A}(\xi, \omega)$. At the end of the input dispersion, the field envelope is given by

$$A(\xi_1, \tau) = \mathcal{F}^{-1}\{\mathcal{A}(0, \omega) \mathcal{G}_1(\xi_1, \omega)\} \quad (47)$$

where \mathcal{F}^{-1} signifies inverse Fourier transformation. The field immediately after the time lens is

$$A(\xi_1 + \epsilon, \tau) = \mathcal{F}^{-1}\{\mathcal{A}(0, \omega) \mathcal{G}_1(\xi_1, \omega)\} H(\tau). \quad (48)$$

Finally, the field envelope at the end of the output dispersion is

$$A(\xi_2, \tau) = \frac{1}{2\pi} \mathcal{F}^{-1} \cdot \{[\mathcal{A}(0, \omega) \mathcal{G}_1(\xi_1, \omega)] * \mathcal{H}(\omega)\} \mathcal{G}_2(\xi_2, \omega) \quad (49)$$

where $\mathcal{H}(\omega)$ is the Fourier transform of the time-lens function and the factor $1/2\pi$ appears because of the convolution theorem. To uncover the full implication of this expression, we begin by expanding the indicated con-

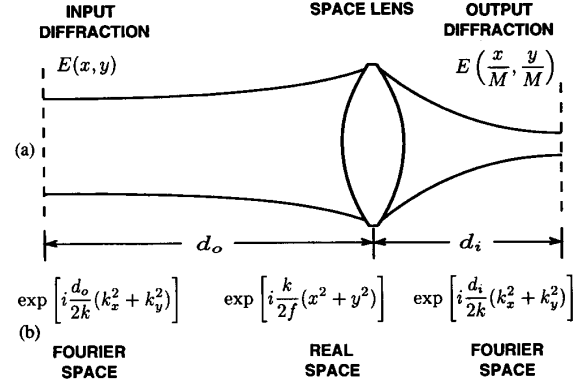


Fig. 7. (a) Configuration for conventional spatial imaging. Output field envelope $E(x/M, y/M)$ is a magnified version of the input field envelope $E(x, y)$ where $M \equiv -d_i/d_o$. (b) Analysis is carried out by cascading the three processes: input diffraction [quadratic phase transformation in Fourier-space variables (k_x, k_y)] \rightarrow lens [quadratic phase transformation in real-space variables (x, y)] \rightarrow output diffraction. Compare with Fig. 6.

volution integral

$$\mathcal{A}(0, \omega) \mathcal{G}_1(\xi_1, \omega) * \mathcal{H}(\omega) = \int_{-\infty}^{\infty} \mathcal{A}(0, \omega') \mathcal{G}_1(\xi_1, \omega') \mathcal{H}(\omega - \omega') d\omega' \quad (50)$$

and substitute it back into (49)

$$A(\xi_2, \tau) = \frac{1}{2\pi} \int_{-\infty}^{\infty} d\omega e^{i\omega\tau} \mathcal{G}_2(\xi_2, \omega) \cdot \frac{1}{2\pi} \int_{-\infty}^{\infty} d\omega' \mathcal{A}(0, \omega') \mathcal{G}_1(\xi_1, \omega') \mathcal{H}(\omega - \omega'). \quad (51)$$

Switching the order of integration and operation on $\mathcal{H}(\omega - \omega')$ we have

$$A(\xi_2, \tau) = \frac{1}{2\pi} \int_{-\infty}^{\infty} d\omega' \mathcal{A}(0, \omega') \mathcal{G}_1(\xi_1, \omega') \cdot \frac{1}{2\pi} \int_{-\infty}^{\infty} d\omega e^{i\omega\tau} \mathcal{G}_2(\xi_2, \omega) \mathcal{H}(\omega - \omega'). \quad (52)$$

Now we can complete the integral over ω on the right-hand side. From Table II

$$\mathcal{H}(\omega - \omega') = \sqrt{4\pi i c} \exp[-ic(\omega - \omega')^2] \quad (53)$$

and the second integral in (52) can be written

$$\begin{aligned} & \sqrt{\frac{ic}{\pi}} \int_{-\infty}^{\infty} \exp(-i\omega^2) \exp[-ic(\omega - \omega')^2] \exp(i\omega\tau) d\omega \\ &= \sqrt{\frac{ic}{\pi}} \exp(-ic\omega'^2) \\ & \cdot \int_{-\infty}^{\infty} \exp[-i\omega^2(b+c)] \exp[i\omega(\tau + 2c\omega')] d\omega \\ &= \sqrt{\frac{c}{(b+c)}} \exp(-ic\omega'^2) \exp\left[\frac{i(\tau + 2c\omega')^2}{4(b+c)}\right]. \end{aligned} \quad (54)$$

The integral was evaluated by noting that it is the inverse Fourier transform of a quadratic phase with a shifted time reference. We can put this result into (52) and write the remaining integral as

$$A(\xi_2, \tau) = \sqrt{\frac{c}{(b+c)}} \exp\left[\frac{i\tau^2}{4(b+c)}\right] \frac{1}{2\pi} \int_{-\infty}^{\infty} \mathcal{A}(0, \omega') \cdot \exp\left[-i\left(a+c-\frac{c^2}{b+c}\right)\omega'^2\right] \cdot \exp\left[i\omega'\left(\frac{c}{b+c}\right)\tau\right] d\omega'. \quad (55)$$

This equation shows us that the output waveform can be found by multiplying the spectrum $\mathcal{A}(0, \omega)$ of the input waveform by a quadratic phase and modifying its time scale.

We are interested in finding the conditions under which the output waveform could reasonably be called an "image" of the input waveform. This would be satisfied if the output waveform had the same envelope profile, but perhaps an altered time scale. If we eliminate the quadratic phase in the integrand of (55), we will obtain this result since the integral represents the inverse Fourier transform of the original waveform spectrum with an altered time scale. Thus, we set $a+c=c^2/(b+c)$ and find that $1/a+1/b=-1/c$. Substituting for a , b , and c from Table II, we have

$$\frac{1}{\xi_1 \frac{d^2\beta_1}{d\omega^2}} + \frac{1}{\xi_2 \frac{d^2\beta_2}{d\omega^2}} = -\frac{\omega_o}{f_T} \quad (56)$$

which is our *temporal-imaging condition*. Note the striking similarity to the lens law $1/d_o+1/d_i=1/f$, which is the spatial-imaging condition. There is a subtle difference, however, in the presence of the minus sign. The origin of this traces back to the nature of the relationship between diffraction and dispersion. In the case of diffraction the instantaneous spatial frequencies of a paraxial beam acquire a negative frequency sweep; the high spatial frequencies travel faster laterally than the low spatial frequencies. On the other hand, for normal dispersion ($d^2\beta/d\omega^2 > 0$), a pulse acquires a positive frequency sweep since the low frequencies travel faster than the high frequencies. Thus, in the sense that a lens counteracts the natural chirping of the medium that precedes it, a time lens must have a different sign of phase curvature than a space lens in order to satisfy the imaging condition.

The possibility of having positive or negative dispersion adds an extra degree of versatility. In the normal lens law, changing the sign of the focal length from positive to negative requires a resultant change in the sign of either the object or image distance to which we ascribe the notion of a virtual object or virtual image. In the temporal-imaging system, however, changing the sign of f_T does not automatically imply the creation of a "temporal virtual image" since (56) could be satisfied by chang-

ing the sign of the dispersion alone and leaving the propagation distance ξ unchanged. This corresponds to a real image formed with a negative lens, a situation that is not possible with real-space lenses since the propagation phenomenon only introduces one sign of dispersion for the spatial Fourier spectrum.

Next, we examine the time-scale factor in the Fourier transform kernel. If we apply the imaging condition (56) to this factor, we find

$$\frac{b+c}{c} = -\frac{b}{a} = -\frac{\xi_2 \frac{d^2\beta_2}{d\omega^2}}{\xi_1 \frac{d^2\beta_1}{d\omega^2}} \equiv M. \quad (57)$$

The time scale is altered by a magnification factor M given by the ratio of the output dispersion to the input dispersion. This expression also has its dual in the spatial domain; the ratio of the image distance to the object distance ($-d_i/d_o$).

Making use of the imaging condition (56) and the definition of the magnification ratio (57), we can finally rewrite (55) as

$$A(\xi_2, \tau) = \frac{1}{2\pi\sqrt{M}} \exp\left[\frac{i\omega_o\tau^2}{2Mf_T}\right] \cdot \int_{-\infty}^{\infty} \mathcal{A}(0, \omega) \exp\left[i\omega\frac{\tau}{M}\right] d\omega = \frac{1}{\sqrt{M}} \exp\left[\frac{i\omega_o\tau^2}{2Mf_T}\right] A\left(0, \frac{\tau}{M}\right). \quad (58)$$

This is the principal result of temporal imaging. It bears a very close resemblance to its spatial counterpart. The output waveform $A(\xi_2, \tau)$ is seen to be a replica of the input waveform scaled in time. In addition, there is a quadratic phase term as one finds in the spatial case [25], and an amplitude scaling $1/\sqrt{M}$ that accounts for energy conservation. We can now add the results of our temporal imaging analysis to Table I.

VIII. RESOLUTION LIMITATIONS

As in any real spatial-imaging system, temporal imaging is subject to the equivalent effects of diffraction due to finite apertures. In this context, the aperture corresponds to a finite time window through which the fields pass on their way through the time lens. In Section VI the concept of a useful aperture time was introduced to limit the time window over which the modulator was principally quadratic. However, in deriving the relations for temporal imaging, we ignored the finite aperture and the effects that it will produce in the image plane. In this section we will consider the effects of a finite time aperture from a slightly different point of view. The reasons are twofold. First, we wish to highlight the linear systems nature of temporal imaging by describing the imaging system in terms of its impulse response. Second, we can take advan-

tage of the concepts of the imaging condition and magnification ratio already derived in the last section (those derivations evolve more naturally when considering an arbitrary input field as opposed to the impulse response point of view).

Our goal is to exploit the linearity of the temporal-imaging system and write the system output in terms of a superposition integral [25]

$$A(\xi, \tau) = \int_{-\infty}^{\infty} h(\tau; \tau_o) A(0, \tau_o) d\tau_o \quad (59)$$

where $h(\tau; \tau_o)$ is the response of the system at time τ to an impulse applied at time τ_o . $A(0, \tau)$ is the input waveform and serves as a weighting function in the integrand.

To find the impulse response, we begin by assuming that the input to the system is an impulse delayed in time by τ_o in the traveling-wave reference frame. Then $A(0, \tau) = \delta(\tau - \tau_o)$ and the fields after the input dispersion are $A(\xi_1, \tau) = G_1(\xi_1, \tau) * \delta(\tau - \tau_o) = G_1(\xi_1, \tau - \tau_o)$. (60)

To model the effect of an aperture, we introduce a pupil function $P(\tau)$ to the time lens so that the transmittance of the time lens becomes $H(\tau)P(\tau)$. In this way we can separate the effects of the quadratic phase from the aperture. Thus, immediately past the time lens the waveform is

$$A(\xi_1 + \epsilon, \tau) = G_1(\xi_1, \tau - \tau_o) H(\tau) P(\tau). \quad (61)$$

Finally, after the output dispersion we have

$$\begin{aligned} h(\tau; \tau_o) &= A(\xi_2, \tau) \\ &= G_1(\xi_1, \tau - \tau_o) H(\tau) P(\tau) * G_2(\xi_2, \tau) \end{aligned} \quad (62)$$

which is the response of the system at time τ due to an impulse at time τ_o . Using the expressions in Table II we can expand the convolution and write

$$\begin{aligned} h(\tau; \tau_o) &= \int_{-\infty}^{\infty} G_1(\xi_1, \tau' - \tau_o) H(\tau') \\ &\quad \cdot P(\tau') G_2(\xi_2, \tau - \tau') d\tau' \\ &= \frac{1}{4\pi i \sqrt{ab}} \int_{-\infty}^{\infty} P(\tau') \exp \left[\frac{i(\tau' - \tau_o)^2}{4a} \right] \\ &\quad \cdot \exp \left[\frac{i\tau'^2}{4c} \right] \exp \left[\frac{i(\tau - \tau')^2}{4a} \right] d\tau' \\ &= \frac{1}{4\pi i \sqrt{ab}} \exp \left[\frac{i}{4} \left(\frac{\tau_o^2}{a} + \frac{\tau^2}{b} \right) \right] \\ &\quad \cdot \int_{-\infty}^{\infty} P(\tau') \exp \left[\frac{i\tau'^2}{4} \left(\frac{1}{a} + \frac{1}{b} + \frac{1}{c} \right) \right] \\ &\quad \cdot \exp \left[\frac{-i\tau'}{2} \left(\frac{\tau_o}{a} + \frac{\tau}{b} \right) \right] d\tau'. \end{aligned} \quad (63)$$

Now, if we invoke the imaging condition derived in the previous section $1/a + 1/b = -1/c$, we can dispense with the quadratic phase term inside the integrand. Thus,

we find that the impulse response is proportional to the Fourier transform of the pupil function in a scaled- and shifted coordinate system, just as in the case of a Fraunhofer diffraction pattern. We can simplify this result a bit more by noting that as this is an impulse response, most of the contribution to $h(\tau; \tau_o)$ will arise from a small region about the point τ_o , and thus, we can replace τ_o with τ/M and the remaining quadratic phase term can be approximated by [25]

$$\begin{aligned} \exp \left[\frac{i}{4} \left(\frac{\tau_o^2}{a} + \frac{\tau^2}{b} \right) \right] &\approx \exp \left[\frac{i}{4} \left(\frac{\tau^2}{aM^2} + \frac{\tau^2}{b} \right) \right] \\ &= \exp \left[\frac{i\omega_o \tau^2}{2Mf_T} \right]. \end{aligned} \quad (64)$$

Making use again of the definition of magnification and rearranging the Fourier transform kernel we can rewrite (63) as

$$\begin{aligned} h(\tau; \tau_o) &= \frac{1}{4\pi i \sqrt{ab}} \exp \left[\frac{i\omega_o \tau^2}{2Mf_T} \right] \\ &\quad \cdot \int_{-\infty}^{\infty} P(\tau') \exp \left[\frac{-i\tau'}{2b} (\tau - M\tau_o) \right] d\tau'. \end{aligned} \quad (65)$$

Now, consider the following change of variables; let $\tilde{\tau} = \tau'/2b$ and $\tau'_o = M\tau_o$. Equation (65) becomes

$$\begin{aligned} h(\tau - \tau'_o) &= \frac{\sqrt{M}}{2\pi} \exp \left[\frac{i\omega_o \tau^2}{2Mf_T} \right] \\ &\quad \cdot \int_{-\infty}^{\infty} P(2b\tilde{\tau}) \exp[-i\tilde{\tau}(\tau - \tau'_o)] d\tilde{\tau} \end{aligned} \quad (66)$$

and we see that in the traveling-wave reference frame, the impulse response is time invariant. Applying the new variables to the superposition integral (59) yields

$$A(\xi_2, \tau) = \int_{-\infty}^{\infty} \frac{h(\tau - \tau'_o)}{M} A\left(0, \frac{\tau'_o}{M}\right) d\tau'_o. \quad (67)$$

With the final definition

$$\tilde{h}(\tau - \tau'_o) = \frac{1}{M} h(\tau - \tau'_o) \quad (68)$$

the impulse response can be written

$$\begin{aligned} \tilde{h}(\tau - \tau'_o) &= \frac{1}{2\pi\sqrt{M}} \exp \left[\frac{i\omega_o \tau^2}{2Mf_T} \right] \\ &\quad \cdot \int_{-\infty}^{\infty} P(2b\tilde{\tau}) \exp[-i\tilde{\tau}(\tau - \tau'_o)] d\tilde{\tau} \end{aligned} \quad (69)$$

and we find

$$A(\xi_2, \tau) = \int_{-\infty}^{\infty} \tilde{h}(\tau - \tau'_o) A\left(0, \frac{\tau'_o}{M}\right) d\tau'_o. \quad (70)$$

Thus, the output waveform from the temporal-imaging system is seen to be a magnified replica of the input waveform convolved with the Fourier transform of the

pupil function (the impulse response). This is what we would expect owing to the duality between the temporal and spatial systems. Substituting b from Table II into the pupil function, we can add the essential form of the impulse response to Table I adjacent to its spatial counterpart.

Note that in the limit of a very large time aperture, the pupil function is approximately unity and the impulse response (69) reduces to

$$\tilde{h}(\tau - \tau'_o) = \frac{1}{\sqrt{M}} \exp \left[\frac{i\omega_o \tau^2}{2Mf_T} \right] \delta(\tau - \tau'_o). \quad (71)$$

From (70) and the sifting theorem, the output waveform then takes the form

$$A(\xi_2, \tau) = \frac{1}{\sqrt{M}} \exp \left[\frac{i\omega_o \tau^2}{2Mf_T} \right] A \left(0, \frac{\tau}{M} \right) \quad (72)$$

in exact agreement with the result from Section VII, (58), where we approached the problem entirely in the frequency domain, with no aperture, and the full-input waveform carried through the calculation.

Finally, let us consider an example from which we can derive a useful rule of thumb. Assume that the pupil function is rectangular in time with an aperture τ_a s long. Then $P(\tau) = \text{rect}(\tau/\tau_a)$ and the impulse response (69) takes the form

$$\tilde{h}(\tau - \tau'_o) = \frac{T}{4\pi b\sqrt{M}} \exp \left[\frac{i\omega_o \tau^2}{2Mf_T} \right] \text{sinc} \left(\frac{\tau_a(\tau - \tau'_o)}{4\pi b} \right). \quad (73)$$

As a rough estimate of the resolution of a time microscope used for expanding fast optical waveforms, we might consider the time to the first zero of the sinc function as a reasonable marker. This corresponds to a time interval in the system output of $(\tau - \tau'_o) = 4\pi b/\tau_a$. It will be much more convenient to translate this into the input time scale, which is accomplished using the magnification ratio M . The input resolution is thus

$$\delta\tau_{\text{in}} = \left| \frac{4\pi b}{M\tau_a} \right| = \frac{4\pi a}{\tau_a}. \quad (74)$$

Now, in most cases of microscopy, the magnification will be large and the image distance will be much greater than the object distance. We may then approximate the object distance as equal to the focal length. In the temporal system this implies that the output dispersion is much greater than the input dispersion or $b \gg a$. Consequently $a \approx -c = -f_T/2\omega_o$ and (74) becomes

$$\delta\tau_{\text{in}} = T_o \frac{f_T}{\tau_a} = T_o f_T^\# \quad (75)$$

where $T_o = 2\pi/\omega_o$ is the period of the optical carrier. This is a very handy expression for estimating the resolution of a temporal-imaging system. As in the case of

spatial imaging, resolution is ultimately governed by the speed of the lens.

For a time lens based on an electrooptic modulator, we can substitute (46) for the f -number and obtain

$$\delta\tau_{\text{in}} = \frac{1}{\Gamma_o f_m}. \quad (76)$$

This is also a convenient expression with a simple interpretation. We know from communication theory that for continuous angle modulation, the product of the peak phase deviation (or modulation index) and the modulating frequency is the peak-frequency deviation that is related to the total spectral bandwidth [27]. For the case of the quadratic time lens, the phase modulation occurs over a small portion of the modulating period and it can be shown that the net bandwidth of the chirped spectrum is simply $\Delta f = \Gamma_o f_m$ and thus $\delta\tau_{\text{in}} = 1/\Delta f$.

It should be emphasized that the steps leading to (74)–(76) relied on the approximation that the time from the peak of the impulse response to the first zero was indicative of the resolution. This does not establish the equivalent of a “Rayleigh criterion” in the time domain, but simply serves as a handy guide. Also, a true rectangular-aperture function is nearly impossible to construct in the time domain because of the bandwidth requirements whereas it is trivial in space. It is interesting, then, to consider the consequences of the myriad possible aperture functions on the resolution of temporal-imaging systems. This is fruitful ground for future study.

IX. CONCLUSIONS

In this paper, we have attempted to lay the foundation for the principles of temporal imaging. The origin of these principles rest in the duality between the problems of paraxial diffraction and narrow-band dispersion. These were constructed on analogous approximations to the relative bandwidths of spatial and temporal Fourier spectra (Fig. 2). The governing differential equations of parabolic form suggest a close relationship to conventional diffusion, but as we have seen, the presence of the imaginary coefficients transformed a problem in stationary dissipation to one of conservative propagation.

Building on the diffraction–dispersion analogy we saw that a quadratic time-phase modulation acts as a time lens to which we can ascribe the equivalent concepts of focal length (now a focal time) and f -number. We believe that these concepts will play a useful role in future discussions and specifications of optical pulse-compression systems.

When we combine dispersion both ahead of and after a time lens, we create the time-domain analog of a spatial-imaging system. Following the implications of the analog, we have derived expressions that relate the output time waveform to the input waveform. When these waveforms have the same overall profile, but possibly an altered time scale, we consider the output to be a time image of the input. The conditions on the strengths of the time lens and the associated dispersions result in the imaging condi-

tion equation (56) that is conceptually identical to the lens law.

Finally, no treatment of imaging is complete without analyzing the resolution limitations. As we would expect, these arise due to the finite aperture or time window through which the optical waveforms must pass. Analysis of the impulse response of the temporal-imaging system reveals that the resolution is related to the Fourier transform of the aperture function (69) and thus is the time-domain equivalent of the Fraunhofer-diffraction pattern. This is an important result and really solidifies the nature of the space-time duality. It also points out the key technological hurdle in making useful temporal-imaging systems. For example, imagine that we wish to construct a time microscope capable of resolving phenomena with 100 fs features. Assume that we can fabricate an electrooptic phase modulator that operates at 50 GHz. What peak phase deviation is necessary to satisfy the 100 fs requirement? Reference to (76) indicates that we must have $\Gamma_0 = 200$ rad, a formidable challenge indeed! Also, note that this time lens has an f -number of only 30 at $\lambda = 1.0 \mu\text{m}$ and thus is not a particularly "fast" lens (a fact that is consistent when the resolution is compared to the carrier period of 3.3 fs).

In closing, we bring to the attention of the reader additional interesting work that is relevant to space-time duality and temporal imaging. This includes matrix approaches to analyzing pulse propagation [28], [29], optical waveform processing [30], [31], self-imaging [32], Fourier transformation [33], and more complex temporal-imaging systems [34, 35].

ACKNOWLEDGMENTS

The author wishes to thank M. Nazarathy and P. Robrish for preliminary stimulating discussions and C. Bennett, R. Scott, and W. Stanton for reading this manuscript and for providing insightful questions and discussions.

REFERENCES

- [1] Since most of the discussion concerning spatial evolution will refer to fields that are laterally confined and thus undergo spreading, we will use "diffraction" to refer to the general problem of propagation. Although we often associate diffraction with wave propagation involving an obstacle such as an edge or an aperture, these objects can be accounted for in the initial field distribution in the Huygens-Fresnel integral and, as such, represent special cases of the general wave propagation problem.
- [2] J. R. Klauder, A. C. Price, S. Darlington, and W. J. Albersheim, "The theory and design of chirp radars," *Bell Syst. Tech. J.*, vol. 39, pp. 745-808, 1960.
- [3] J. A. Giordmaine, M. A. Duguay, and J. W. Hansen, "Compression of optical pulses," *IEEE J. Quantum Electron.*, vol. QE-4, pp. 252-255, 1968.
- [4] D. Grischkowsky, "Optical pulse compression," *Appl. Phys. Lett.*, vol. 25, pp. 566-568, 1974.
- [5] J. E. Bjorkholm, E. H. Turner, and D. B. Pearson, "Conversion of cw light into a train of subnanosecond pulses using frequency modulation and the dispersion of a near-resonant atomic vapor," *Appl. Phys. Lett.*, vol. 26, pp. 564-566, 1975.
- [6] J. K. Wigmore and D. R. Grischkowsky, "Temporal compression of light," *IEEE J. Quantum Electron.*, vol. QE-14, pp. 310-315, 1978.
- [7] E. B. Treacy, "Optical pulse compression with diffraction gratings," *IEEE J. Quantum Electron.*, vol. QE-5, pp. 454-458, 1969.
- [8] D. Grischkowsky and A. C. Balant, "Optical pulse compression based on enhanced frequency chirping," *Appl. Phys. Lett.*, vol. 41, pp. 1-3, 1982.
- [9] R. L. Fork, C. H. Brito Cruz, P. C. Becker, and C. V. Shank, "Compression of optical pulses to six femtoseconds by using cubic phase compensation," *Opt. Lett.*, vol. 12, pp. 483-485, 1987.
- [10] M. Haner and W. S. Warren, "Generation of programmable, picosecond-resolution shaped laser pulses by fiber grating pulse compression," *Opt. Lett.*, vol. 12, pp. 398-400, 1987.
- [11] M. Haner and W. S. Warren, "Synthesis of crafted optical pulses by time domain modulation in a fiber-grating compressor," *Appl. Phys. Lett.*, vol. 52, 1988.
- [12] B. H. Kolner, "Active pulse compression using an integrated electro-optic phase modulator," *Appl. Phys. Lett.*, vol. 52, pp. 1122-1124, 1988.
- [13] A. A. Godil, B. A. Auld, and D. M. Bloom, "Time-lens producing 1.9 ps optical pulses," *Appl. Phys. Lett.*, vol. 62, pp. 1047-1049, 1993.
- [14] S. A. Akhmanov, A. S. Chirkin, K. N. Drabovich, A. I. Kovrigin, R. V. Khokhlov, and A. P. Sukhorukov, "Nonstationary nonlinear optical effects and ultrashort light pulse formation," *IEEE J. Quantum Electron.*, vol. QE-4, pp. 598-605, 1968.
- [15] S. A. Akhmanov, A. P. Sukhorukov, and A. S. Chirkin, "Nonstationary phenomena and space-time analogy in nonlinear optics," *Sov. Phys.—JETP*, vol. 28, pp. 748-757, 1969.
- [16] A. Papoulis, *Systems and Transforms with Applications in Optics*. New York: McGraw-Hill, 1968.
- [17] L. S. Telegin and A. S. Chirkin, "Reversal and reconstruction of the profile of ultrashort light pulses," *Sov. J. Quantum Electron.*, vol. 15, pp. 101-102, 1985.
- [18] S. A. Akhmanov, V. A. Vysloukh, and A. S. Chirkin, "Self-action of wave packets in a nonlinear medium and femtosecond laser pulse generation," *Sov. Phys.—Usp.*, vol. 29, pp. 642-677, 1987.
- [19] B. H. Kolner and M. Nazarathy, "Temporal imaging with a time lens," *Opt. Lett.*, vol. 14, pp. 630-632, 1989.
- [20] W. J. Caputi, "Stretch: A time transformation technique," *IEEE Trans. Aerospace Electron. Syst.*, vol. AES-7, pp. 269-278, 1971.
- [21] H. A. Haus, *Waves and Fields in Optoelectronics*. Englewood Cliffs, NJ: Prentice-Hall, 1984.
- [22] A. E. Siegman, *Lasers*. Mill Valley, CA: University Science, 1986, pp. 339-343.
- [23] G. B. Whitham, *Linear and Nonlinear Waves*. New York: Wiley, 1974.
- [24] P. W. Berg and J. L. McGregor, *Elementary Partial Differential Equations*. San Francisco, CA: Holden-Day, 1966.
- [25] J. W. Goodman, *Introduction to Fourier Optics*. New York: McGraw-Hill, 1968.
- [26] B. H. Kolner, "Active pulse compression," in *Ultrafast Phenomena IV*. Kyoto, Japan. Berlin: Springer-Verlag, 1988.
- [27] F. G. Stremler, *Introduction to Communication Systems*. Reading, MA: Addison-Wesley, 1977.
- [28] A. G. Kostenbauder, "Ray-pulse matrices: A rational treatment for dispersive optical systems," *IEEE J. Quantum Electron.*, vol. 26, pp. 1148-1157, 1990.
- [29] S. P. Dijaali, A. Dienes, and J. S. Smith, "ABCD-matrices for dispersive pulse propagation," *IEEE J. Quantum Electron.*, vol. 26, pp. 1158-1164, 1990.
- [30] A. W. Lohmann and D. Mendlovic, "Temporal perfect shuffle optical processor," *Opt. Lett.*, vol. 17, pp. 822-824, 1992.
- [31] ———, "Temporal filtering with time lenses," *Appl. Opt.*, vol. 31, pp. 6212-6219, 1992.
- [32] T. Jansson and J. Jansson, "Temporal self-imaging effect in single-mode fibers," *J. Opt. Soc. Amer.*, vol. 71, pp. 1373-1376, 1981.
- [33] T. Jansson, "Real-time Fourier transformation in dispersive optical fibers," *Opt. Lett.*, vol. 8, pp. 232-234, 1983.
- [34] I. P. Christov, "Design of a compound time lens," *J. Mod. Opt.*, vol. 36, pp. 1027-1030, 1989.
- [35] I. P. Christov, "Theory of a time telescope," *Opt. Quantum Electron.*, vol. 22, pp. 473-480, 1990.

Brian H. Kolner, photograph and biography not available at the time of publication.